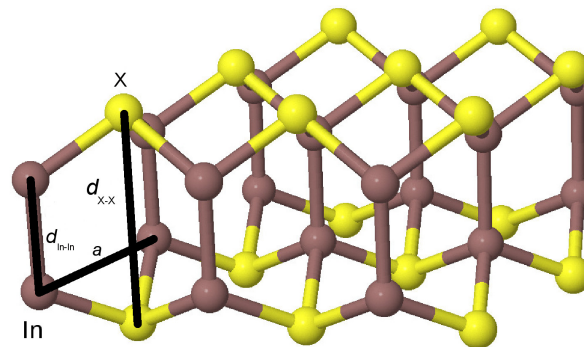# Electronic and Vibrational Properties of Monolayer Hexagonal Indium Chalcogenides

V. Zólyomi, N. D. Drummond and V. I. Fal'ko

Department of Physics, Lancaster University

QMC in the Apuan Alps IX, TTI, Tuscany, Italy

Friday 1st August, 2014

Introduction: Gallium and Indium Chalcogenides

- **Two-dimensional materials**: graphene, hexagonal boron nitride, silicene, germanane, a variety of transition metal dichalcogenides, gallium chalcogenides, . . .

- **New members of the family**: **gallium chalcogenides** (Ga_2S_2, Ga_2Se_2 and Ga_2Te_2) and **indium chalcogenides** (In_2X_2, In_2Se_2 and In_2Te_2). We will focus on the latter.

- Indium chalcogenides take a wide variety of forms, including tetragonal, rhombohedral, cubic, monoclinic, orthorhombic and **hexagonal** phases.

- Indium selenide (InSe) exists in a layered hexagonal structure in nature with an in-plane lattice parameter of 4.05 Å and vertical lattice parameter of 16.93 Å.
  - InSe has been proposed for use in ultrahigh-density electron-beam data storage.
  - Very recently, Ajayan and coworkers at Rice University and Los Alamos have succeeded in producing samples of few-layer (4–11 layers) hexagonal InSe by mechanical exfoliation.

- Indium sulphide (InS) and indium telluride (InTe) exhibit orthorhombic and tetragonal structures, respectively, but it may be possible to prepare a hexagonal structure.

Structure of α Indium Chalcogenides

- Structure of α-In$_2$X$_2$ monolayers:

  - Viewed from above, the monolayer forms a 2D **honeycomb lattice**.
  - Vertically aligned In$_2$ and X$_2$ pairs at hexagonal A and B sublattice sites.
  - The In atoms in each In$_2$ dimer are bound together, and each In atom is bound to the neighbouring X atoms.
  - Distance between the atoms within each X$_2$ pair is considerably larger.
  - D_{3h} point group (includes $z \to -z$ reflectional symmetry).
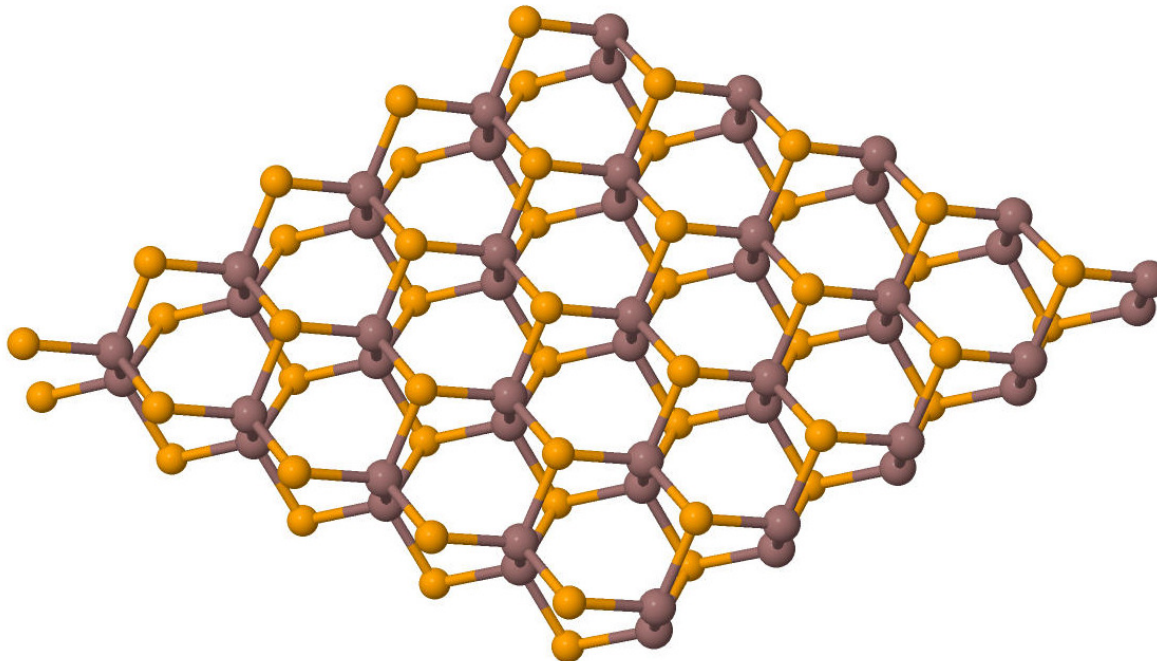
Structure of β Indium Chalcogenides

- Structure of β-In$_2$X$_2$ monolayers:

  - Vertically aligned In$_2$ dimers are located at hexagonal A sublattice sites.
  - One layer of X atoms is located at the B sublattice sites.
  - The other layer of X atoms is located at the C sublattice sites.
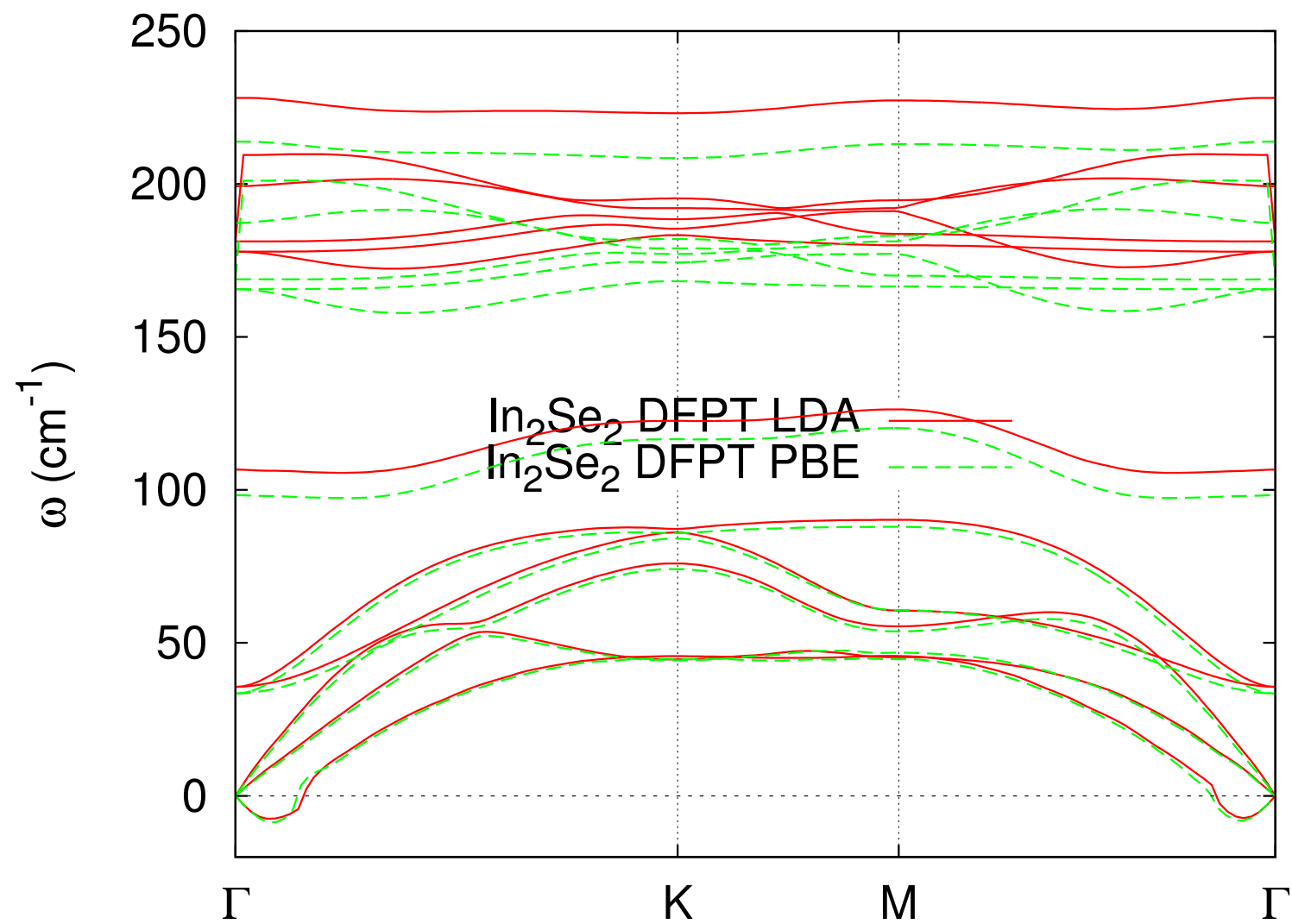 - D_{3d} point group (includes inversion symmetry).
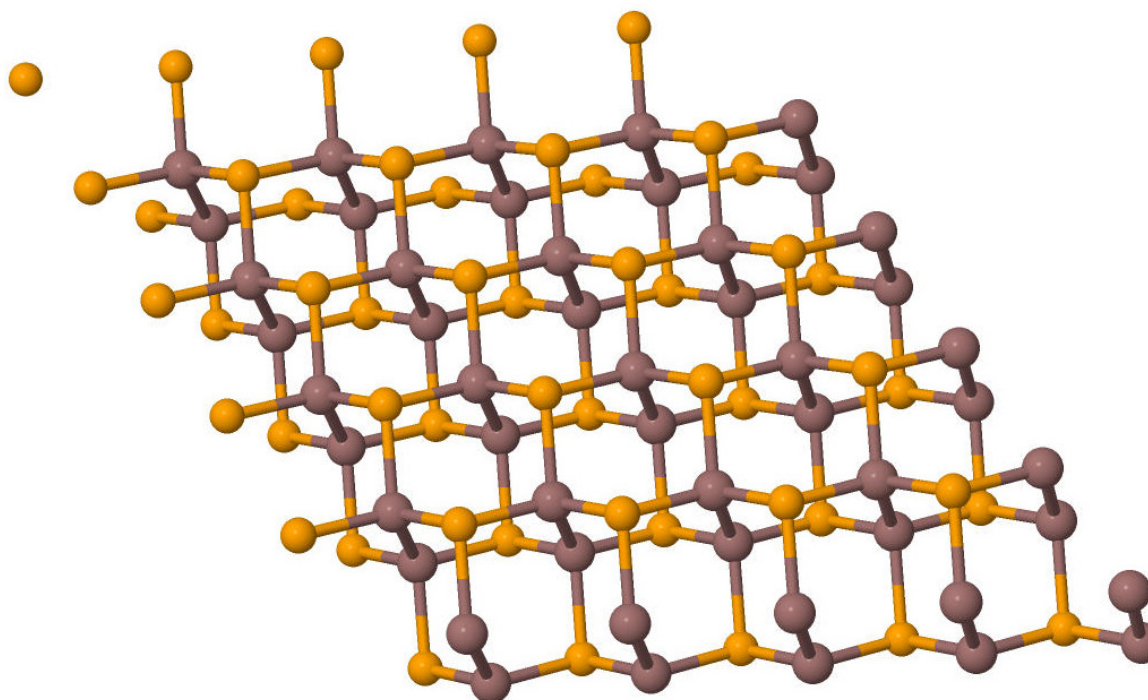
Computational Methodology and Structural Parameters

- Density functional theory using the CASTEP and VASP plane-wave-basis codes.

  - LDA, PBE and HSE06 functionals (latter only for calculating the band structure).
  - Phonon dispersion curves calculated using both finite displacements and density functional perturbation theory.

- Experimental lattice parameter of bulk hexagonal InSe: $a = 4.05$ Å.

  - C.f., for monolayer α-In$_2$Se$_2$, $a = 3.95$ and 4.09 Å according to the LDA and PBE functionals, respectively.
  - LDA bond lengths are systematically smaller than the PBE bond lengths.

- Lattice parameters increase with the atomic number of the chalcogen, while the In–In bond lengths hardly change.
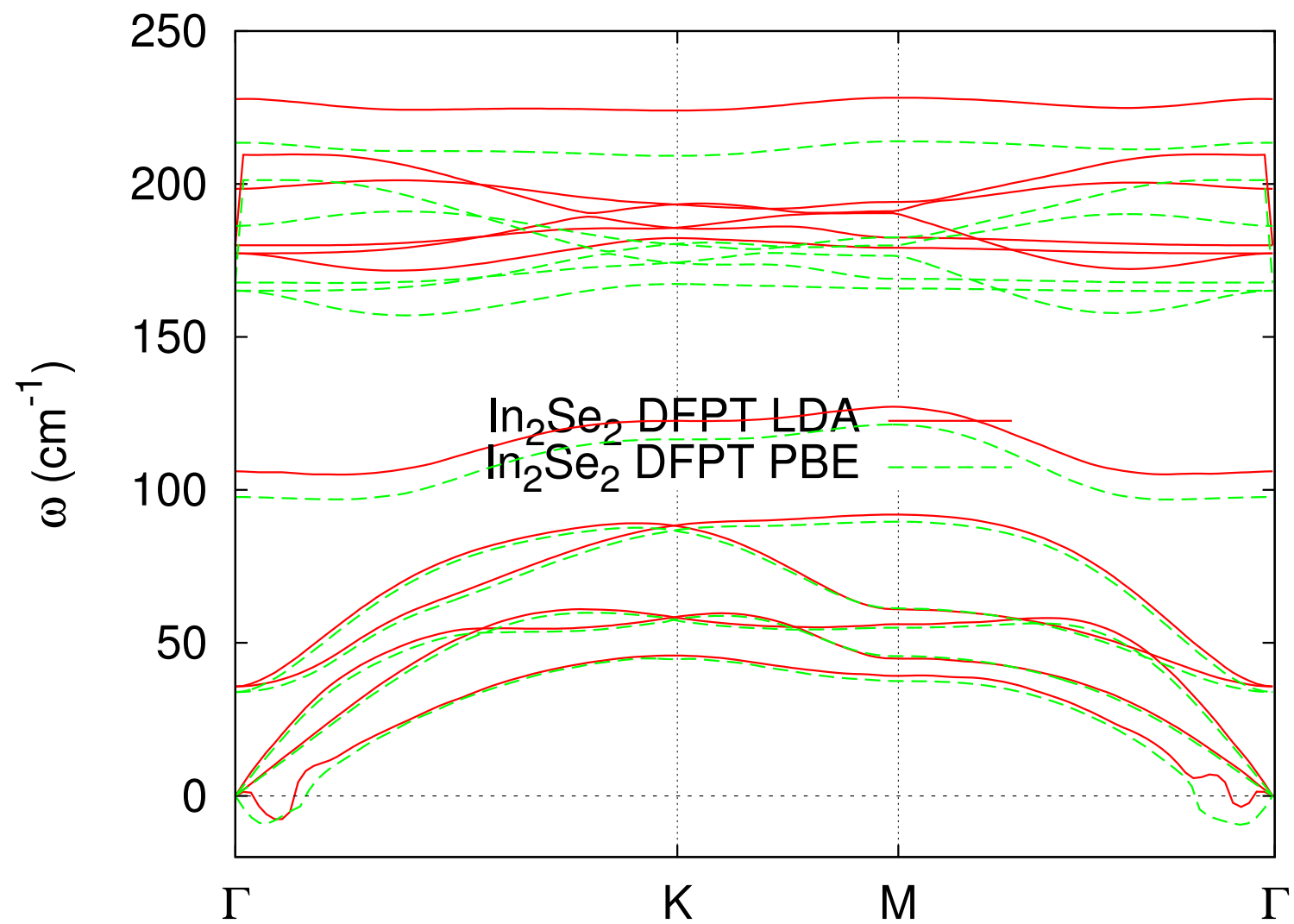
Cohesive (Atomisation) Energy

- Cohesive energy E_c: energy of two isolated indium atoms plus the energy of two isolated chalcogen atoms minus the energy per unit cell of the In_2X_2 layer.

  - Difference between LDA and PBE cohesive energies is significant; nevertheless, both predict the cohesive energy to be largest for In_2S_2 and smallest for In_2Te_2.
  - The β structures are dynamically stable, but the static-lattice cohesive energy is slightly less than that of the α structures (by 0.022 and 0.013 eV per unit cell according to the LDA and PBE functionals, respectively).
  - *Very small energy difference between the structures.*
  - Inclusion of phonon zero-point energy makes no difference to this conclusion.
  - There is almost certainly a significant energy barrier between the two structures.
  - Might find domains of the two structures in samples.

α-**In$_2$Se$_2$ Phonon Dispersion Curve**

In$_2$Se$_2$ DFPT LDA
In$_2$Se$_2$ DFPT PBE

ω (cm^{-1})

250
200
150
100
50
0

Γ K   M Γ

β-In$_2$Se$_2$ Phonon Dispersion Curve

In$_2$Se$_2$ DFPT LDA

In$_2$Se$_2$ DFPT PBE

ω (cm^{-1})

Γ K   M Γ

Lattice Dynamics

- We find no imaginary phonon frequencies, other than a small pocket near Γ.

  - Small pocket of instability: ubiquitous problem in first-principles calculations for 2D materials. Difficult to converge the flexural (ZA) branch.
  - Isolated atomic crystals of hexagonal indium chalcogenides (both α and β phases) are **dynamically stable**.

- The nonanalytic contribution to the dynamical matrix due to long-range Coulomb interactions (longitudinal/transverse optic mode splitting) is neglected in this work.

- The PBE functional predicts softer phonons than the LDA.

- Infrared and Raman spectroscopy: zone-centre optic phonons allow experimental classification of these materials.

  - A normal mode is infrared active if it affects the **dipole moment**.
  - A normal mode is Raman active if it affects the **polarisability**.

Analysis of Zone-Centre LDA Optical Phonons For α-In$_2$X$_2$

Branch	Γ-pt. freq. (cm^{-1})			Irrep.	IR int. (D^{2}Å^{-2}amu^{-1})			Raman activity
	In$_2$S$_2$	In$_2$Se$_2$	In$_2$Te$_2$		In$_2$S$_2$	In$_2$Se$_2$	In$_2$Te$_2$	
4	40.6	35.6	30.7	E''	–	–	–	$E_z \leftrightarrow E_\parallel$
5	40.6	35.6	30.7	E''	–	–	–	$E_z \leftrightarrow E_\parallel$
6	135	107	85.4	A_1'	–	–	–	$\begin{cases} E_\parallel \leftrightarrow E_\parallel \\ E_z \leftrightarrow E_z \end{cases}$
7	262	178	146	E''	–	–	–	$E_z \leftrightarrow E_\parallel$
8	262	178	146	E''	–	–	–	$E_z \leftrightarrow E_\parallel$
9 (TO)	264	181	150	E'	10.2 ($E_\parallel$)	5.18	3.57	$E_\parallel \leftrightarrow E_\parallel$
10 (LO)	264	181	150	E'	10.2 ($E_\parallel$)	5.18	3.57	$E_\parallel \leftrightarrow E_\parallel$
11 (ZO)	282	199	162	A_2''	0.25 (E_z)	0.10	0.061	–
12	293	228	207	A_1'	–	–	–	$\begin{cases} E_\parallel \leftrightarrow E_\parallel \\ E_z \leftrightarrow E_z \end{cases}$

- Experimental resonant Raman frequencies of few-layer InSe: 115 cm^{-1} (A_1'), 179 cm^{-1} (E''), 187 cm^{-1} (A_2''), 201 cm^{-1} (A_2''), 212 cm^{-1} (E') and 227 cm^{-1} (A_1').

- Experimental non-resonant Raman frequencies of few-layer InSe: 117 cm^{-1} (A_1'), 179 cm^{-1} (E'') and 227 cm^{-1} (A_1').

Analysis of Zone-Centre LDA Optical Phonons For β-In$_2$X$_2$

Branch	Γ-pt. freq. (cm^{-1})			Irrep.	IR int. (D^{2}Å^{-2}amu^{-1})			Raman activity
	In$_2$S$_2$	In$_2$Se$_2$	In$_2$Te$_2$		In$_2$S$_2$	In$_2$Se$_2$	In$_2$Te$_2$	
4	40.8	35.8	31.2	E_g	–	–	–	$\begin{cases} E_{\parallel} \leftrightarrow E_{\parallel} \\ E_{\parallel} \leftrightarrow E_z \end{cases}$
5	40.8	35.8	31.2	E_g	–	–	–	$\begin{cases} E_{\parallel} \leftrightarrow E_{\parallel} \\ E_{\parallel} \leftrightarrow E_z \end{cases}$
6	134	106	84.9	A_{1g}	–	–	–	$\begin{cases} E_{\parallel} \leftrightarrow E_{\parallel} \\ E_z \leftrightarrow E_z \end{cases}$
7	261	177	146	E_g	–	–	–	$\begin{cases} E_{\parallel} \leftrightarrow E_{\parallel} \\ E_{\parallel} \leftrightarrow E_z \end{cases}$
8	261	177	146	E_g	–	–	–	$\begin{cases} E_{\parallel} \leftrightarrow E_{\parallel} \\ E_{\parallel} \leftrightarrow E_z \end{cases}$
9 (TO)	262	180	149	E_u	10.4 ($E_{\parallel}$)	5.4	3.8	–
10 (LO)	262	180	149	E_u	10.4 ($E_{\parallel}$)	5.4	3.8	–
11 (ZO)	281	198	161	A_{2u}	0.25 (E_z)	0.10	0.06	–
12	293	228	207	A_{1g}	–	–	–	$\begin{cases} E_{\parallel} \leftrightarrow E_{\parallel} \\ E_z \leftrightarrow E_z \end{cases}$

- The frequencies are very similar in the two polytypes.

- Two modes are Raman-active in the α structure but not the β structure: **means of distinguishing the phases**.

# α-In$_2$Se$_2$ Band Structure
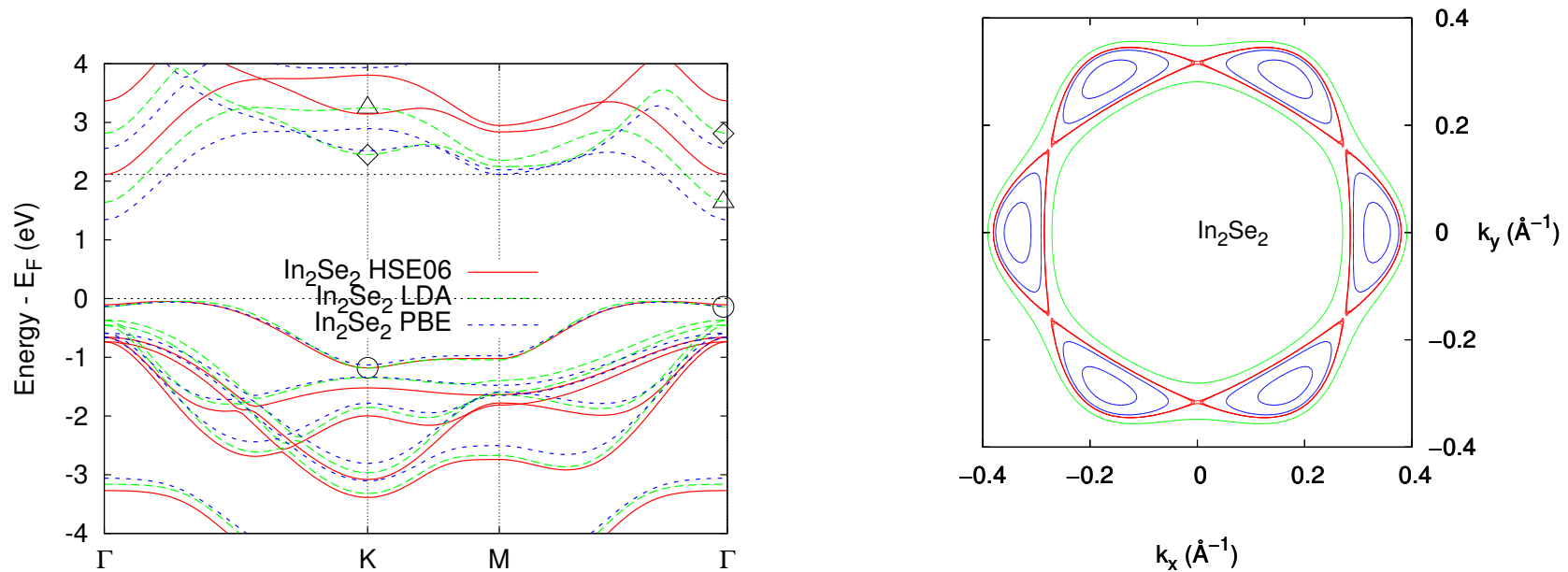
- The LDA bands around the Fermi level are dominated by s- and p-type orbitals.

- Interband absorption selection rules:

    - Photons polarised in-plane are absorbed by transitions between bands whose wave functions have the same $z \to -z$ symmetry (even→even and odd→odd);
    - Photons polarised along the z axis cause transitions between bands with opposite symmetry (even→odd and odd→even).

In$_2$X$_2$ Electronic Band Structures

- In$_2$S$_2$, In$_2$Se$_2$ and In$_2$Te$_2$: indirect-gap semiconductors, with the valence-band maximum (VBM) lying between Γ and K.

- The valence band has a saddle point on the Γ–M line.

  - Lifshitz transition: when the hole concentration reaches the critical value where all states are empty above the saddle point, the Fermi-surface topology changes.
  - Carrier density at which Lifshitz transition takes place was found by integrating the DFT density of states from the saddle point to the valence-band edge.

- Valence band near VBM can be fitted by an inverted-Mexican-hat-shaped polynomial

$$\mathcal{E}_{\mathrm{VB}}(\mathbf{k}) = \sum_{i=0}^{3} a_{2i}k^{2i} + a_6' k^6 \cos(6\phi),$$


where ϕ is measured from the Γ–K line.
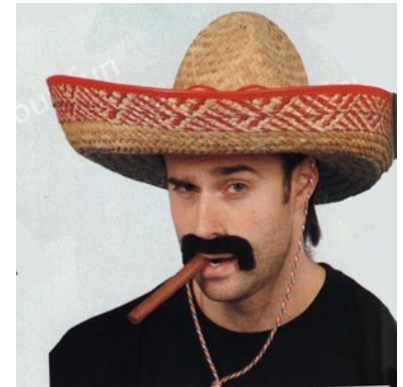
α-In$_2$X$_2$ Band Gaps, Spin-Splitting and Effective Masses (I)

	Gap (eV)	$|\Delta E_{\mathrm{SO}}^{\mathrm{K}}|$ (meV)		Elec. eff. mass m^*/m_e				n_{Lifshitz} (10^{13} cm^{-2})
		VB	CB	Γ^c	K^c	M$^c_{\to\Gamma^c}$	M$^c_{\to\mathrm{K}^c}$	
α-In$_2$S$_2$	2.53	18	79	0.26	0.86	1.24	0.42	8.32
α-In$_2$Se$_2$	2.16	92	23	0.20	0.71	2.30	0.33	6.00
α-In$_2$Te$_2$	2.00	13	47	0.17	0.53	0.64	0.23	8.14

- The conduction-band minimum (CBM) is at the Γ point in all cases except the LDA band structure of α-In$_2$Te$_2$, where it is at the M point.

- There are local minima of the conduction band at Γ, K and M in each case, with the exception of the PBE band structure of α-In$_2$Te$_2$.

- Experimental gap of few-layer InSe (from photoconductivity spectra): 1.4 eV.
  - Not much higher than the measured gap of bulk InSe (1.2 eV).
  - Differs from GaX, where the gap increases significantly in few-layer samples.
  - *Lower* than monolayer DFT-LDA gap (1.68 eV)!
  - Possibilities: difference between few-layer and monolayer In$_2$X$_2$ gaps; large excitonic effects; few-layered sample contained a different structure.

α-In$_2$X$_2$ and β-In$_2$X$_2$ Electronic Band Structures

- β-In$_2$X$_2$ is also an indirect gap semiconductor.

  – The valence band is inverted-Mexican-hat-shaped around Γ, with the maximum on the Γ–K line and a saddle point on the Γ–M line.
  – The conduction band minimum is at Γ.
  – Behaviour of conduction band at K and M is different, however.
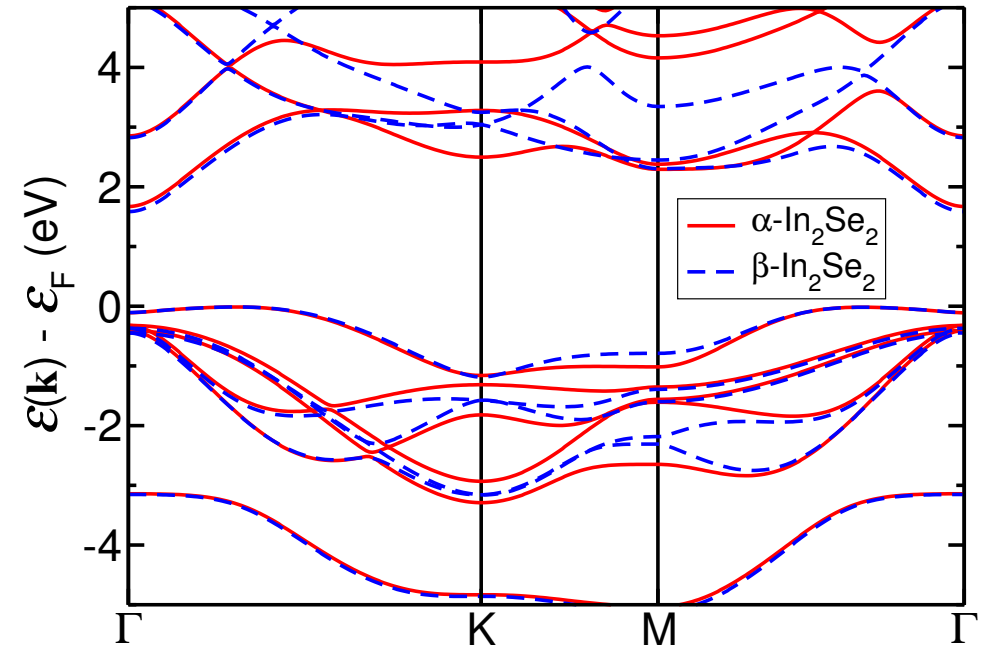
- β-In$_2$X$_2$ gaps are smaller than α-In$_2$X$_2$ gaps by about 0.1 eV.

- Some of the bands exhibit spin splitting, including the highest valence ($\Delta E_{\mathrm{SO}}^{v,\mathrm{K}}$) and lowest conduction ($\Delta E_{\mathrm{SO}}^{c,\mathrm{K}}$) bands near the K point.

In$_2$Se$_2$ Optical Absorption Spectra
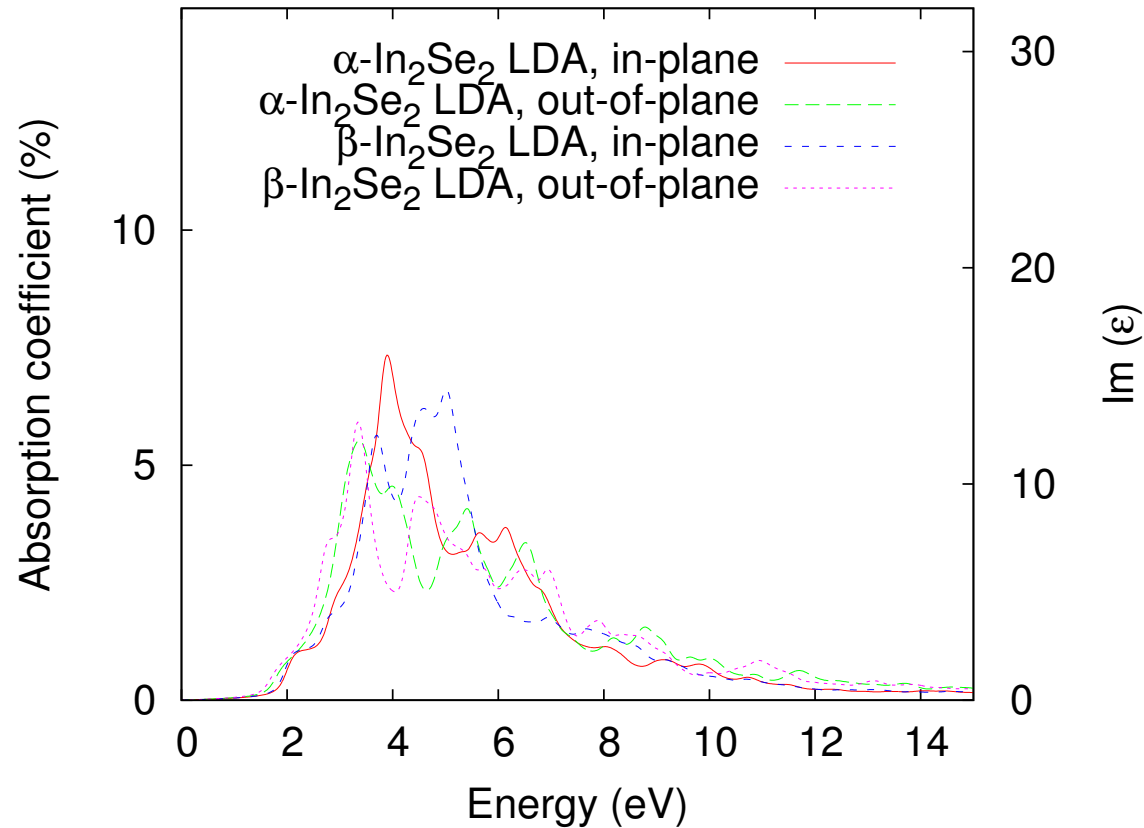
- Absorption shows a prominent peak (originating from the vicinity of the K point) at 3–5 eV, where the absorption coefficient of In$_2$Se$_2$ is similar to that of graphene.

  - *Ultrathin films of InX biased in vertical tunnelling transistors with graphene electrodes could be used as an active element for the detection of UV photons.*

Conclusions

- DFT indicates that the 2D hexagonal indium chalcogenides In_2S_2, In_2Se_2 and In_2Te_2 are dynamically stable, indirect-band-gap semiconductors with an unusual inverted-Mexican-hat-shaped valence band.

- We have provided the phonon frequencies and Raman and IR activities of modes, to assist the identification of these structures.

- Two possible structures (α and β) were investigated, which are very close in energy.

- Saddle points in the valence band along the Γ–M line lead to a Lifshitz transition in the event of hole doping, for which we have calculated the critical carrier density.

- We have given a qualitative description of the optical absorption spectra, which suggest that atomically thin films of indium chalcogenides could find application in ultraviolet photon detectors.

To-Do (Where QMC Finally Gets a Mention)

- *Study bulk InX and GaX, to understand stacking effects in the multilayer samples that experimentalists are currently actually working with.*

  - Two polytypes for each layer: α and β. Can invert/reflect these to give α' and β'.
  - Two stacking arrangements for In_2 or Ga_2 dimers: AA and AB.
  - The **five** AA-stacked structures: $\alpha\alpha$, $\alpha\alpha'$, $\alpha\beta$, $\beta\beta$ and $\beta\beta'$.
  - The **six** AB-stacked structures: $\alpha\alpha$, $\alpha\alpha'$, $\alpha\beta$, $\alpha'\beta$, $\beta\beta$ and $\beta\beta'$.
  - Different exchange–correlation functionals and dispersion-correction schemes give different relative energies on an energy scale of more than ~ 0.02 eV per cell.
  - *Use QMC to identify the most stable structures.*
  - Problem: the In and Ga pseudopotentials from the CASINO library don't work at all in CASTEP and hence CASINO. Ghost states due to Kleinman–Bylander representation? Use DFT pseudopotentials?
  - *Determine the Raman/IR-active phonon modes to help the experimentalists.*

- *Use DMC to investigate the quasiparticle gaps and exciton binding energies.*

  - DMC and GW_0 studies of hexagonal BN indicate that the latter underestimates the quasiparticle gap by more than 1.5 eV (and G_0W_0 is even worse).

Acknowledgements